Proc. Natl. Acad. Sci. USA
Vol. 95, pp. 15177–15182, December 1998
Biochemistry

Structure of a biological oxygen sensor: A new mechanism for heme-driven signal transduction

WEIMIN GONG*, BING HAO*, SHEREF S. MANSY*†, GONZALO GONZALEZ*†, MARIE A. GILLES-GONZALEZ*†‡, AND MICHAEL K. CHAN*§¶

Departments of *Biochemistry and §Chemistry and the †Plant Biotechnology Center, The Ohio State University, 484 West 12th Avenue, Columbus, OH 43210

Communicated by Max F. Perutz, Medical Research Council, Cambridge, United Kingdom, October 26, 1998 (received for review October 2, 1998)

ABSTRACT **The FixL proteins are biological oxygen sensors that restrict the expression of specific genes to hypoxic conditions. FixL's oxygen-detecting domain is a heme binding region that controls the activity of an attached histidine kinase. The FixL switch is regulated by binding of oxygen and other strong-field ligands. In the absence of bound ligand, the heme domain permits kinase activity. In the presence of bound ligand, this domain turns off kinase activity. Comparison of the structures of two forms of the *Bradyrhizobium japonicum* FixL heme domain, one in the "on" state without bound ligand and one in the "off" state with bound cyanide, reveals a mechanism of regulation by a heme that is distinct from the classical hemoglobin models. The close structural resemblance of the FixL heme domain to the photoactive yellow protein confirms the existence of a PAS structural motif but reveals the presence of an alternative regulatory gateway.**

An increasing number of biological sensors are being discovered that monitor the presence of physiologically important gases by way of heme cofactors. These include the FixL protein of *Rhizobia*, the soluble guanylyl cyclase of vertebrates, and the CooA protein of *Rhodospirillum rubrum* that sense O_2, NO, and CO, respectively (1–3). The signaling mechanisms of these heme-based sensors are of considerable interest, since they must ultimately regulate DNA binding or enzymatic activities. The FixL protein has especially broad relevance because this modular protein contains a histidine kinase domain belonging to the large class of two-component regulatory systems, whereas the heme-binding sensory domain belongs to the PAS-domain superfamily (1, 4–8).

PAS domains occur in many sensory proteins spanning all three major kingdoms of life: *Bacteria, Archaea,* and *Eukarya* (8–10). These domains contain a small number of conserved amino acids within a sequence of about 90 residues. Several PAS-domain proteins are known to detect their signal by way of an associated cofactor (1, 11, 12). The only available structure of a PAS domain is that of the small photoactive yellow protein (PYP), which has been proposed as a prototype for a conserved PAS fold (9, 12). If the PYP fold is a prototype, then how does the same fold bind cofactors as varied as heme, flavin, or a 4-hydroxycinnamyl chromophore and use them to detect oxygen, redox, or light? (1, 11, 12). Does signal detection induce an analogous rearrangement of the domain in every case? Must this sensory domain interact with a structurally conserved class of transmitter domains or proteins? Comparisons of the structures of several PAS domains in their activating and inactivating conformations, together with knowledge of their cognate transmitters, should shed light on these questions.

The heme domain of FixL regulates a histidine kinase domain that transduces its signal by a conserved phosphoryl transfer mechanism (5, 6). Deoxy-FixL (Fe^{2+}), but not oxy-FixL ($Fe^{+2}O_2$), autophosphorylates at a histidine with a γ-phosphate from ATP. In *Rhizobia,* the transfer of this phosphoryl group to the transcription factor FixJ triggers a cascade of gene expression required for nitrogen fixation (4, 13, 14). A spin-state switching mechanism has been proposed for FixL regulation, in which binding of strong-field ligands to the heme iron inactivates the kinase (15). Consistent with this mechanism, cyanide inactivates ferric FixL proportionately to the saturation of the heme with this ligand and in a manner analogous to the oxygen inactivation of ferrous FixL.

We have determined the three-dimensional structures of the met (Fe^{3+}), "on," and cyanomet ($Fe^{3+}CN^-$), "off", forms of a monomeric 14.9-kDa *Bradyrhizobium japonicum* FixL heme domain (BjFixLH) by x-ray crystallography. These structures reveal a novel heme-binding fold and biological mechanism for sensing of physiological heme ligands. They shed light on the versatility of the PAS motif as a switching mechanism in signal transduction systems and the interactions that occur between this class of sensory domains and the histidine kinase transmitter domains.

MATERIALS AND METHODS

Overexpression and Protein Purification. Codons 141–270 of the *B. japonicum fixL* gene *(BjfixLH)* were amplified in a PCR with pRJ7349 as the template (16). A 5′*Nde*I-3′*Hin*dIII *BjfixLH* fragment without polymerization error was cloned into a P_{tac}-based expression vector (17). *Escherichia coli* strain TG1 carrying this plasmid, pBH32, was induced as described previously for the full-length gene (1). BjFixLH protein from a 33%–45% saturated ammonium sulfate cut of a cleared lysate was further purified on a Sephacryl S-100 gel filtration column (Pharmacia) equilibrated in 20 mM Tris·HCl, pH 8.0/5% glycerol/50 mM NaCl, at 4°C. Purity was confirmed by gel electrophoresis and an A_{280}/A_{395} absorbance ratio = 0.23 for met-BjFixLH.

Crystallization and Data Collection. Crystals of met-BjFixLH were grown at 4°C in 4.5 M NaCl/5% 2-methyl-2,4-pentanediol (vol/vol)/0.1 M Hepes buffer (pH 7.5) by way of

Abbreviations: BjFixLH, *Bradyrhizobium japonicum* FixL heme domain; MAD, multiwavelength anomalous diffraction; PAS, an acronym formed from the names of the first proteins recognized as sharing this sensory motif, i.e., the *p*eriod clock protein of *Drosophila*, the *a*ryl hydrocarbon receptor nuclear translocator of vertebrates, and the *s*ingle-minded protein of *Drosophila*; PYP, photoactive yellow protein.

Data deposition: The atomic coordinates have been deposited in the Protein Data Bank, Biology Department, Brookhaven National Laboratory, Upton, NY 11973 [PDB ID codes 1BV6 (met-BjFixLH) and 1BV5 (cyanomet-BjFixLH)].

¶To whom reprint requests should be addressed. e-mail: chan@chemistry.ohio-state.edu.

‡To whom reprint requests should be addressed at Plant Biotechnology Center, The Ohio State University, 1060 Carmack Road, Columbus, OH 43210-1002. e-mail: gilles-gonzalez.1@osu.edu.

The publication costs of this article were defrayed in part by page charge payment. This article must therefore be hereby marked "*advertisement*" in accordance with 18 U.S.C. §1734 solely to indicate this fact.

Table 1. Summary of crystallographic results

Data collection						Phasing statistics, 3.0 Å			
Data set	λ, Å	Res., Å	R_{sym}, %*†	Reflections, observed/unique	Completeness, %†	Phasing power, iso/ano	R_{cullis}	R_{kraut}	Figure of merit
Nat1	1.7396	2.7	8.1 (23.2)	29279/5002	95.3 (97.0)	—/2.33	–	0.014	0.411
Nat2	1.7379	2.9	6.7 (23.5)	18123/4098	95.7 (97.9)	—/1.08	–	0.068	0.254
Nat3	1.6984	2.8	8.0 (25.4)	25616/4504	95.2 (98.5)	1.02/1.64	–	0.047	0.351
Nat4	1.4938	2.4	7.6 (22.1)	31111/7104	97.0 (98.0)	1.38/—	0.664	0.073	0.265
Pt	1.4938	2.9	8.8 (18.4)	18929/3605	84.4 (87.4)	0.99/—	0.711	0.095	0.222
CN	1.6984	2.7	4.9 (21.5)	19321/4402	83.7 (87.5)				
Total									0.656

Refinement

Data set	met-BjFixLH	cyanomet-BjFixLH
Resolution range, Å	20.0–2.4	20.0–2.7
Total number of non-hydrogen atoms	1063	1026
Number of water molecules	82	51
$R_{crystal}$‡ (R_{free})§ (%)	19.9 (24.8)	18.9 (26.1)
RMS bond length deviation	0.014 Å	0.012 Å
RMS bond angle deviation	1.675°	1.683°

*R_{sym} (I) = $\Sigma_h\Sigma_i|I_i - I|/\Sigma_h\Sigma_i I$, where I is the mean intensity of the i observations of reflection h.
†Numbers in parentheses represent the statistics for the shell comprising the outer 10% (theoretical) of the data.
‡$R_{crystal} = 100 \times \Sigma|F_{obs} - F_{calc}|/\Sigma|F_{obs}|$, where F_{obs} and F_{calc} are the observed and calculated structure factors, respectively.
§R_{free} is the same as $R_{crystal}$, calculated using 8% of the data excluded from refinement.

the vapor diffusion method and achieved their final size within 1 month. Crystals of a platinum derivative were obtained by soaking native crystals with a mixture of 5 mM di-μ-iodobis(ethylenediamine)diplatinum (II) nitrate and 5 mM potassium tetracyanoplatinate for 4 days. Cyanomet-BjFixLH crystals were obtained by treating the met-BjFixLH crystals with cyanide (5 h in 10 mM KCN/4.5 M NaCl/5% 2-methyl-2, 4-pentanediol/0.1 M Hepes buffer at pH 7.5); within several minutes, the color of the crystals changed from orange red (met-BjFixLH) to cherry red (cyanomet-BjFixLH). Before data collection, the crystals were transferred stepwise to solutions of reservoir buffer containing increasing amounts of glycerol up to a maximal concentration of 40% (vol/vol). The crystals were lifted onto small nylon loops at the end of mounting pins and cooled at 100 K in a stream of nitrogen.

Diffraction data were collected at beamline X4A at the National Synchrotron Light Source in Brookhaven, NY, by using a RAXIS 100 detector. The crystals belong to the space group R32 with unit cell dimensions a = b = 128.8 Å, c = 58.9 Å, and one BjFixLH per asymmetric unit. Multiwavelength anomalous diffraction (MAD) data were collected at four different wavelengths, corresponding to the inflection point of the Fe edge (1.7386 Å), the maximum of the peak above the edge (1.7379 Å), and two remote points at higher energy (1.6984 Å and 1.4938 Å). Pt and cyanomet-BjFixLH data were collected at the remote wavelengths. Data processing and reduction were performed by using DENZO and SCALEPACK (18).

Structure Determination and Refinement. The crystallographic results are summarized in Table 1. The phases were determined by using the program PHASES (19) by a combination of MAD phasing at the iron edge to take advantage of the mononuclear iron site, and isomorphous and anomalous phasing from a platinum derivative. Both the MAD and derivative data were required to obtain interpretable maps. The heme iron site was located from the Nat2 anomalous Patterson map and confirmed from the Nat3-Nat1 difference Patterson map. MAD phasing was carried out by treating the data as multiple isomorphous replacement and anomalous datasets: native with native anomalous scattering (Nat1-ano), derivative anomalous (Nat2-ano), and derivative isomorphous with anomalous scattering (Nat3-iso, Nat3-ano, Nat4-iso, and Nat4-ano). For the platinum derivative, three Pt sites with low occupancy were located by difference Fourier methods by using the initial MAD phase and then were included in the final phase calculation and refinement. The phases were further improved by solvent flattering with the PHASES program. At this stage, the electron density was clear enough to locate the heme and trace most of the backbone.

The model building and structure refinement were carried out by the programs O and X-PLOR (20, 21). Eight percent of the data were set aside for calculation of the free-R factor (22). The first residues at the N terminus of the met-BjFixLH were not observed and are presumably disordered. A flat bulk solvent correction and an overall anisotropic B-factor scaling were applied to the data. Solvent molecules were found from the 3σ Fo-Fc map. Pro 195 was found to be a cis-proline. The structure of cyanomet-BjFixLH was solved by using the refined met-BjFixLH model. The Fo-Fc map revealed obvious structural shifts from residues 211 to 215 and additional density in the distal heme pocket consistent with cyanide binding. The structures of met- and cyanomet-BjFixLH were determined to 2.4 Å and 2.7 Å resolution, respectively, assessed by using the program PROCHECK (23). All stereochemical parameters were within the acceptable ranges. Figures were prepared with the programs XTALVIEW (24), MOLSCRIPT (25), and RASTER 3D (26).

RESULTS AND DISCUSSION

The Protein Fold. Unlike the more commonly studied classes of heme proteins (myoglobin, cytochrome *c*, cytochrome P450 CAM) that are mainly α-helical, the dominant structural feature of the FixL heme domain is a five-stranded antiparallel β barrel (Figs. 1 and 2). The overall fold of BjFixLH can be described as a left-handed glove that encloses a heme cofactor. The fingers are formed primarily from the β barrel (residues 155–168 and 235–255), the palm from α-helical loops (residues 170–215), and the thumb from β sheets (residues 220–234). The only distortion from the closed hand is the C-terminal helix that protrudes from one of the fingers of the β barrel and leads into the kinase domain. This glutamine-rich helix corresponds to the region often called the Q-linker. The heme is cusped within the left side of the glove. This fold may help to explain the ubiquitous nature of PAS domains over a wide variety of kingdoms and sensory systems.

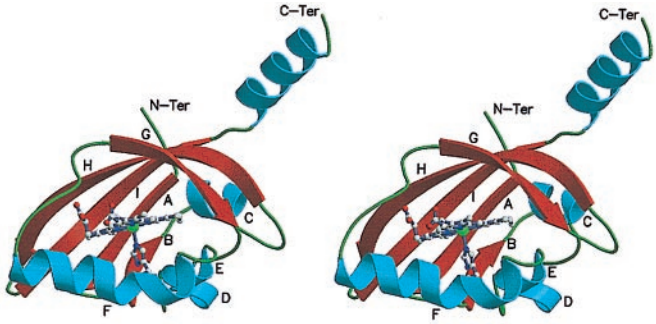

FIG. 1. Ribbons diagram of BjFixLH. The secondary structure elements are color-coded with α-helices as blue, β-sheets as red, and random coils as green. The atoms of the heme cofactor and the proximal histidine are shown as ball-and-stick models and are colored by their elements, with carbon as gray, nitrogen as blue, oxygen as red, and iron as green.

Just as a hand can enclose a variety of objects, the PAS fold appears able to accommodate many chemically diverse cofactors.

The Heme Pocket. Met-BjFixLH contains a pentacoordinate heme iron, with the imidazole side chain of His 200 providing its axial ligand and no other ligands coordinating the heme. As expected for pentacoordinate hemes, the porphyrin ring appears significantly puckered. The heme propionate six hydrogen bonds to the backbone NH's of residues 214–216, and the heme propionate seven forms salt bridges with the side chains of His 214 and Arg 220. The heme pocket is primarily hydrophobic. Residues Val 188, Met 192, Tyr 203, and Ile 204 help to orient the His 200 on the proximal side of the heme. Two additional residues on the same side, Ile 159 and Leu 191, are more peripheral. The side chains of Ile 157, Phe 176, Gly 224, Phe 249, and Tyr 207 lie in the same plane as the porphyrin ring. The distal side is defined by Ile 215, Leu 236, Ile 238, Val 222, Met 234, and Ile 216.

The ligand binding site is hydrophobic but fairly accessible by means of an entryway marked by three water residues that interact with Arg 220. The hydrophobic interior near the ligand binding site is bounded by the side chains of Leu 236 and Ile 238 on β sheet H_β, and by Ile 215. Comparison of the BjFixLH structure with myoglobins and hemoglobins reveals considerable differences in the protein secondary structures overall and the regions surrounding the heme. Hence, one would predict little or no similarity in their binding sites. Remarkably, alignment of the central heme and the bound histidine of BjFixLH and *Glycera dibranchiata* hemoglobin, which also has a distal (E7) leucine instead of the more common histidine, reveals some surprising similarities (Fig. 3) (27). Two of the hydrophobic groups on a β strand within the distal pocket of BjFixLH, Leu 236, and Ile 238 are positioned analogously to Leu 58 (E7) and Val 62 (E11) of *G. dibranchiata* hemoglobin, respectively. The other residue in BjFixLH that is close enough to interact with bound ligands, Ile 215, is part of a critical loop involved in the regulatory signal. The presence of this additional residue results in a slightly smaller hydrophobic distal pocket for BjFixLH. The close similarity of the relative orientations of the histidine ligand and the two distal side chains, in these two clearly evolutionarily distant oxygen binding proteins, raises the question whether there are also electronic effects associated with oxygen binding that nature is able to exploit. Consistent with these observations, the ligand binding pocket of the nitric-oxide transport protein from a blood-sucking insect also reveals these features (Fig. 3) (28). When their coordinated histidines are oriented similarly, Leu 236 and Ile 238 in BjFixLH occupy positions similar to Leu 123 and Leu 133, respectively, in the NO transport protein. However, the side chain residue of Leu 123 in the NO transport protein is farther away from the metal than Leu 236 in BjFixLH. This difference may reflect the different functional ligands for the two proteins.

Influence of the Heme Pocket Structure on Ligand Binding. The highly apolar heme binding pocket in FixL is consistent with spectroscopic and ligand binding properties that are in some respects much simpler than those of most myoglobins (17, 29–33). Because there are no polar side chains within hydrogen bonding distance of the ligand, stabilization from polar residues does not contribute to the binding energy. Although the oxygen affinities of FixLs are in the range expected for an apolar distal heme pocket, the association and dissociation rate constants are vastly slower (34, 35). Nitric oxide, whose binding kinetics are also governed primarily by the reactivity of the heme iron, binds slowly to FixL (Table 2). In contrast, imidazole, whose association rate is principally determined by steric access, binds very rapidly to FixL (32). The coupling of FixL's ligand binding properties to its regu-

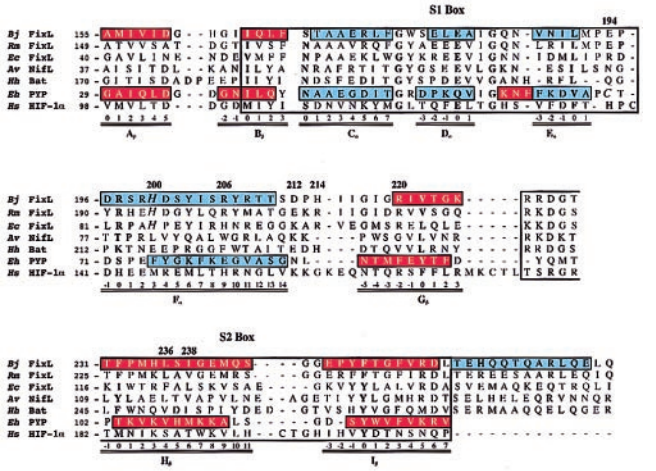

FIG. 2. Sequence alignment of selected PAS-domain proteins from *Bacteria, Archaea*, and *Eukarya*. The sequences correspond to the FixLs from *B. japonicum* (*Bj* FixL), *Rhizobium meliloti* (*Rm* FixL), and *E. coli* (*Ec* FixL), the NifL flavoprotein from *Azotobacter vinelandii* (*Av* NifL), the bacterio-opsin activator protein from *Halobacterium halobium* (*Hh* Bat), the PYP from *Ectothiorhodospira halophila* (Eh PYP), and the hypoxia-inducible factor-1α from humans (Hs HIF-1α) (4, 8, 9, 16, 38, 39). The S1 and S2 boxes (large boxes), conserved PAS-domain residues (bold type), sites of cofactor attachment (italics), α-helices (blue), and β-sheets (red) are shown. The secondary-structure assignments for met- and cyanomet-BjFixLH were determined by PROCHECK and DSSP (23, 40). The proposed naming scheme for secondary-structure regions is indicated below the alignment. The FixL sequences illustrate the conservation of residues specific to the regulatory mechanism. The other proteins were chosen to illustrate the ubiquity of the PAS fold in *Bacteria*, *Archaea*, and *Eukarya*, and the diversity of its functions and cofactors.

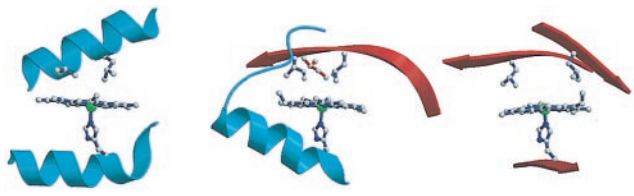

FIG. 3. Ball-and-stick diagrams of three heme-binding pockets. Structures are shown for *Glycera dibranchiata* hemoglobin (PDB ID: 2HBG) (*Left*), BjFixLH (*Center*), and the NO transporter protein (PDB ID: 1NP1) (*Right*) (27, 28). The rightmost and leftmost side chains correspond to the E7 and E11 residues of hemoglobins, respectively. The additional side chain in BjFixLH (red) corresponds to Ile 215. The structures were aligned based on the orientation of the proximal histidine and the porphyrin ring. The atoms are colored as in Fig. 1.

Table 2. Comparison of the ligand binding parameters of FixL to those of the wild-type sperm whale myoglobin and its Val (E7) and Leu (E7) mutants*

	O_2			NO	Imidazole
	k_{on}, $\mu M^{-1}s^{-1}$	k_{off}, s^{-1}	K_d, μM	k_{on} (Fe^{2+}), $\mu M^{-1}s^{-1}$	k_{on}, $M^{-1}s^{-1}$
BjFixL†	0.14	20	140	0.73	16000
H64V SWMb‡	110	9900	91	270	54000
H64L SWMb‡	98	4100	43	190	5200
Wild-type SWMb‡	16	14	0.83	22	160

*All measurements were at pH 7.0 and 20 or 25°C.
†FixL O_2, NO, and imidazole binding data are from Gilles-Gonzalez *et al.* (17); unpublished results of R. Eich, G. Gonzalez, and J. S. Olson, and Mansy *et al.* (32), respectively.
‡Sperm whale myoglobin (SWMb) O_2, NO, and imidazole binding data are from Quillin *et al.* (34), Eich *et al.* (41), and Mansy *et al.* (32), respectively.

latory function would account for these kinetics if the intermediates are high in energy. In such intermediates the binding state would be changed but the protein would not yet have rearranged.

Relation to PAS Domains. The FixL heme binding region overlaps a PAS domain (8). A characteristic feature of these domains is two conserved regions termed the S1 and S2 boxes that were first identified from their sequence homology (Fig. 2). This work describes the first structure of a sensory domain having both boxes. The structure of PYP, which contains only the S1 box sequence motif, has been put forth as a structural prototype for the PAS domain family (9, 12). Indeed, comparison of BjFixLH and PYP reveals significant structural homology within their PAS domains (Fig. 4).

A sequence alignment of the FixL and PYP proteins based on their structural homology is depicted in Fig. 2. The conserved residues that characterize the PAS domains are not involved in the regulatory mechanism for either protein. We suggest that it is likely that these residues act to stabilize the conserved PAS fold. The only interaction of conserved PAS-motif residues in BjFixLH is a salt bridge formed by the side chains of Glu 182 and Arg 226, which reside in the S1 box and S2 box, respectively. Because this salt bridge sits over the critical region of the PYP regulatory gateway, we looked carefully for changes in the orientations of these side chains in the "on" and "off" structures of BjFixLH, but we found none. Although the second β sheet (I_β) of the S2 box leads into the C-terminal α-helix and hence to the kinase domain, no significant structural differences were found within the S1 and S2 boxes of met- and cyanomet-BjFixLH.

Although PYP appears to lack the S2 box based on sequence homology, it is structurally similar to BjFixLH (Fig. 4). One structural difference is within a loop (GH) located between two β sheets (residues 225–231 in BjFixLH, residues 97–102 in PYP). Another difference is that a region of BjFixLH (residues 141–151) that corresponds to the N-terminal cap of PYP (residues 1–25) appears disordered. This disorder may be a consequence of starting the FixL heme domain sequence somewhat later than the analogous PYP sequence. Alternatively, it may reflect a structural difference between the N termini of the two proteins, since BjFixLH shares no conserved motif with PYP over this region. The largest differences, however, occur between residues 189 and 219 of BjFixLH and the corresponding residues 63 to 91 of PYP. This region is localized around the central helix F_α (residues 196–210 in BjFixLH and residues of 75–85 in PYP) and arises because of the different cofactors and signaling gateways used by the two proteins. The chromophore in PYP and the heme in BjFixLH are separated by 9 Å and lie on opposite sides of the F_α helix. This helix in BjFixLH is significantly shifted relative to PYP because of insertion of the heme that it coordinates at His 200. The regions preceding this helix, residues 63–69 in PYP (189–194 in BjFixLH), form part of the binding pocket of the PYP chromophore. The loop following this helix (residues 211–219 in BjFixLH and 86–91 in PYP) forms the signaling gateway in BjFixLH. These results point to the importance of the central helix F_α and the loops that flank it as being the critical regulatory region for the PAS domain family. It appears that the remainder of the PAS fold forms the structural scaffold.

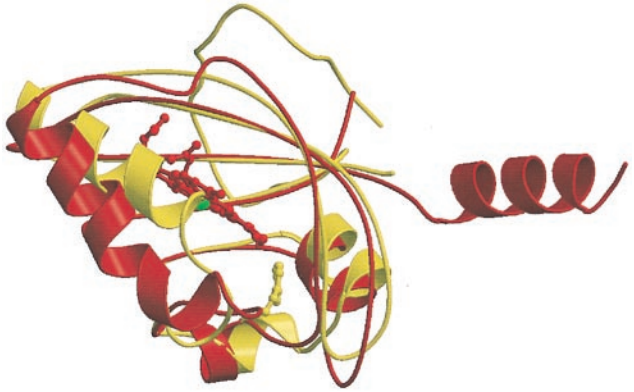

FIG. 4. Comparison of the tertiary structures of the two PAS-domain prototypes. BjFixLH (red) and PYP (PDB ID: 2PHY) (yellow) together with their heme and hydroxycinnamate cofactors, respectively, are shown.

Proposed Nomenclature for PAS Superfamily. The strong structural homology of BjFixLH and PYP, two proteins with distinctly different sequences, confirms the existence of a prototypical fold for the PAS domain (Fig. 4). The secondary-structure elements are clearly conserved. The β barrel and the α-helices form a conserved structural fold with only the major helix F_α being shifted in different proteins to accommodate various cofactors and signaling mechanisms. To facilitate discussion, we propose a new nomenclature for the PAS family based on the structural features of these proteins. By analogy to hemoglobins, we suggest that the amino acid residues should be associated with their location in the conserved regions of secondary structures as shown in Fig. 2, with the secondary structural elements labeled A_β, B_β, C_α, D_α, E_α, F_α, G_β, H_β, and I_β (36). Each loop would be defined by the secondary structures that flank it (e.g., loop AB). Residues within regions of secondary structure are numbered with respect to the most conserved residue in that feature. The advantage of this scheme is that it greatly facilitates discussion about structural similarity. For example, the first S1 box residue, Ile 165 in BjFixLH and Ile 39 in PYP, would be residue $B_\beta 0$ in both structures. Similarly, the critical regulatory region could be described for all the PAS proteins as the EFG core.

Mechanism of Signal Transduction. Ultimately it is the molecular mechanism by which FixL transduces its ligand binding signal that is of greatest interest. To resolve this mechanism, we have solved the structures of both met- and cyanomet-BjFixLH. For technical reasons, we chose to compare the ferric species for our initial studies, although the likely species in *B. japonicum* is ferrous FixL, and the physiological

ligand is oxygen or possibly nitric oxide (17). The redox state does not appear to affect the signaling mechanism. Cyanide induces the same signaling response, and its affinity ($K_d \approx 10^{-6}$ M) for the heme iron is in fact greater than that of oxygen ($K_d \approx 10^{-4}$ M for BjFixLH) (15, 31).

Comparison of the met and cyanomet forms shows distinct changes within this heme-binding domain. Whereas the hydrophobic side chains of Leu 236 ($H_\beta 4$) and Ile 238 ($H_\beta 6$), on the distal side of the heme iron, shift to accommodate the bound cyanide, the main-chain positions and the orientation of the β strand H_β do not change. A third residue, Ile 215, lies to the side of the ligand binding site and is part of the critical loop involved in the regulatory mechanism. This residue shifts slightly when the ligand binds.

The largest changes occur in the FG loop region (Ser 211 to Ile 215) at the surface of the protein (Fig. 5). The driving force for these changes appears to be a flattening of the porphyrin ring on binding of cyanide. This flattening is transmitted to the protein by means of the interactions between the heme propionates and the Nδ1 ring and main-chain nitrogens of His 214. This residue is conserved in all FixLs as histidine or arginine, either of which has a protonated nitrogen that can form a salt bridge to one of the heme propionates. As the heme becomes more planar, the propionates move downward, pushing the histidine ≈1.6 Å away from the heme, thereby initiating the protein conformational change.

An interesting feature of this change is that, whereas the movement of the porphyrin is small, it is sufficient to shift the interaction of His 214 to a different carboxylate oxygen of heme propionate 7. In met-BjFixLH, the His 214 Nδ1 forms a salt bridge primarily to the propionate O1A, whereas in cyanomet-BjFixLH, this same nitrogen interacts solely with the propionate O2A. The orientation of the carboxylate in met-BjFixLH is fixed by a salt bridge between O2A and Arg 220, a residue that is conserved in all FixL proteins. The propionate O1A also hydrogen bonds to a water molecule. Residue His 214 is clearly important to this mechanism of induced conformational change. This histidine is oriented away from the carboxylate of the heme propionate and must push the main chain with it when it shifts its position.

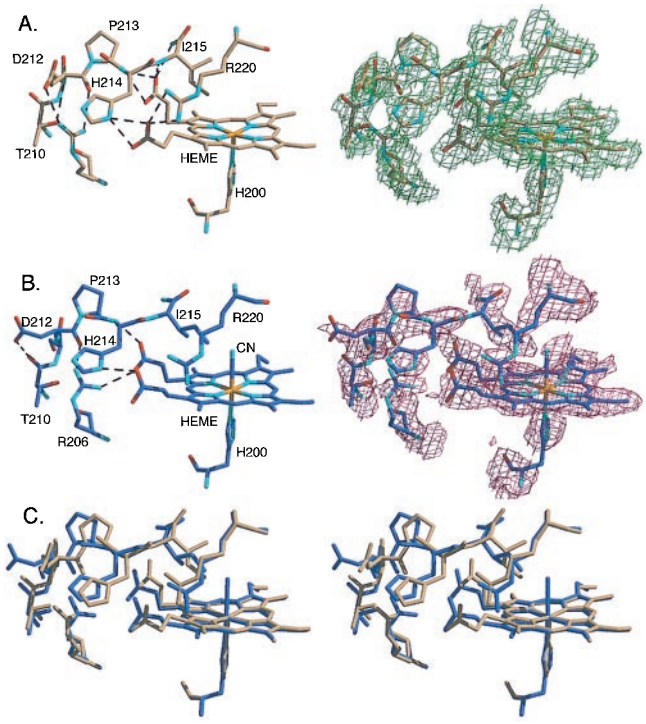

FIG. 5. Comparison of the structures of the regulatory FG loop of BjFixLH in the unliganded "on" and cyanide bound "off" states. *(A)* The structure of the FG loop in the met-BjFixLH (brown) illustrating the hydrogen-bonding interactions (*Left*) and $2F_O$-F_C electron density map (1σ) (*Right*). *(B)* Corresponding figure for cyanomet-BjFixLH (blue) showing hydrogen bonding (*Left*) and electron density (*Right*). *(C)* Stereoview of overlap of the refined models for both states.

The contribution of heme propionate 6 to the conformational change is more subtle. Hydrogen bonding of the O1D propionate oxygen shifts from the main-chain NH groups of residues 214–216 to the main-chain NH groups of only His 214. The O2D propionate oxygen, which hydrogen bonds the main-chain NH of His 214 and water in met-BjFixLH, shifts its interaction to the Nδ1 of Arg 206 ($F_\alpha 9$), as well as a water, in cyanomet-BjFixLH.

The next important residue in the molecular signaling mechanism is Arg 206 ($F_\alpha 9$). The position of this well-conserved arginine influences the position of Asp 212, which undergoes the largest conformational change of all the side chains. In met-BjFixLH, Arg 206 forms hydrogen bonding and ionic interactions with the main-chain carbonyl and side-chain carboxylate of Asp 212, respectively. In cyanomet-BjFixLH, Arg 206 maintains its hydrogen bond to the Asp 212 main-chain carbonyl, but it can no longer form a salt bridge to the Asp 212 carboxylate because of its interaction with the heme propionate 6. Because of the loss of the salt bridge to Arg 206, Asp 212 rotates around its Cα-Cβ bond so as to form a hydrogen bond to the backbone carbonyl of Thr 210 ($F_\alpha 13$).

Based on the localized conformational changes between the "on" and "off" states of BjFixLH, one possible model for the signaling mechanism is that the kinase domain interacts with the heme domain around the FG regulatory loop. This interaction would be the most straightforward way for the conformational signal to be transduced from the sensory domain to the kinase domain. Although the C-terminal α-helix in the BjFixLH structure is relatively far from the regulatory loop region, the location of this helix may be a consequence of crystal packing forces. By shifting the helix upward toward the rest of the protein, it may be possible to bring the kinase domain sufficiently close to interact with the regulatory loop. Because the full-length *B. japonicum* FixL protein exists as a dimer, however, it is more likely that the kinase domain of one subunit interacts with the regulatory loop of its partner (17).

The met- and cyanomet-BjFixLH structures suggest a gateway for signal transfer significantly different from that of the other structurally determined PAS prototype, PYP (12). Based on the PYP structure, one would predict that the conformational change should occur in the EF loop (residues 189–195 in FixL). This region is quite distant from the structurally determined BjFixLH regulatory site, the FG loop (residues 211–215 in BjFixLH). The sequence alignments of PAS proteins indicate that the FG loop is one of the least conserved regions in the PAS domain (8). This loop is shorter in PYP than in the vast majority of other PAS-domain proteins, including FixL. Thus this region, whose variability is at least partly responsible for PYP's poor match in the S2 box, may be the site of signal transduction for the larger family of PAS-domain proteins.

The structure of PYP has led some to speculate, by analogy to many signaling systems, that the regulatory region of PYP is a signal-dependent dimerization site (9). The degree of conservation of that region lends some support to this notion. For example, a tyrosine residue occurs in many PAS proteins at a site where a critical arginine occurs in PYP. It is also possible that, as proposed for FixL, the regulatory domain of PYP interacts with a transmitter. These possibilities will require further study. Given the great versatility of PAS-domain-cofactor interactions, their regulatory aspects need not be universally shared or mutually exclusive.

To our knowledge, this study reveals a new mechanism for the initiation of a conformational change by a heme center. In

both hemoglobin and FixL, binding of strong-field ligands leads to a spin-state change and a motion of the heme iron that necessitates compensatory changes in other parts of the protein (15, 36, 37). Unlike hemoglobin, where movement of the axial histidine ligand induces the well-known allosteric changes, in FixL the axial ligand is rigidly held. It is the flattening of the porphyrin itself that triggers the changes in conformation. Hence, the FixL proteins represent a distinct class of heme proteins in terms of fold, function, and mechanism. The FixL heme domain, along with PYP, provides structural prototypes for the PAS-domain superfamily. Given that PAS domains are frequently associated with kinase domains of the class found in FixL, the mechanisms of signal transduction discovered for the FixL heme domain structure should have broad relevance.

We thank Dr. Muttaiya Sundaralingam for the use of his RAXIS machine for the initial crystal screening experiments and Dr. Craig Ogata for beamline assistance. The X4A beamline at the National Synchrotron Light Source, a Department of Energy facility, is supported by the Howard Hughes Medical Institute. This research was supported by grant MCB9724048 from the National Science Foundation (to M.A.G.-G.), grant AI40575-02 from the National Institutes of Health (to M.K.C.), and funds from The Ohio State University.

1. Gilles-Gonzalez, M. A., Ditta, G. & Helinski, D. R. (1991) *Nature (London)* **350,** 170–172.
2. Garbers, D. L. & Lowe, D. G. (1994) *J. Biol. Chem.* **269,** 30741–30744.
3. Shelver, D., Kerby, R. L., He, Y. & Roberts, G. P. (1997) *Proc. Natl. Acad. Sci. USA* **94,** 11216–11220.
4. David, M., Daveran, M.-L., Batut, J., Dedieu, A., Domergue, O., Ghai, J., Hertig, C., Boistard, P. & Kahn, D. (1988) *Cell* **54,** 671–683.
5. Parkinson, J. S. & Kofoid, E. C. (1992) *Annu. Rev. Genet.* **26,** 71–112.
6. Gilles-Gonzalez, M. A. & Gonzalez, G. (1993) *J. Biol. Chem.* **268,** 16293–16297.
7. Monson, E. K., Weinstein, M., Ditta, G. S. & Helinski, D. R. (1992) *Proc. Natl. Acad. Sci. USA* **89,** 4280–4284.
8. Zhulin, I. B., Taylor, B. L. & Dixon, R. (1997) *Trends Biochem. Sci.* **22,** 331–333.
9. Pellequer, J.-L., Wager-Smith, K. A., Kay, S. A. & Getzoff, E. D. (1998) *Proc. Natl. Acad. Sci. USA* **95,** 5884–5890.
10. Nambu, J. R., Lewis, J. O., Jr., Wharton, K. A. & Crews, S. T. (1991) *Cell* **67,** 1157–1167.
11. Hill, S., Austin, S., Eydmann, T., Jones, T. & Dixon, R. (1996) *Proc. Natl. Acad. Sci. USA* **93,** 2143–2148.
12. Genick, U. K., Borgstahl, G. E. O., Ng, K., Ren, Z., Pradervand, C., Burke, P. M., Srajer, V., Teng, T.-Y., Schildkamp, W. & McRee, D. F. (1997) *Science* **275,** 1471–1475.
13. Reyrat, J.-M., David, M., Blonski, C., Boistard, P. & Batut, J. (1993) *J. Bacteriol.* **175,** 6867–6872.
14. Agron, P. G., Ditta, G. S. & Helinski, D. R. (1993) *Proc. Natl. Acad. Sci. USA* **90,** 3506–3510.
15. Gilles-Gonzalez, M. A., Gonzalez, G. & Perutz, M. F. (1995) *Biochemistry* **34,** 232–236.
16. Anthamatten, D. & Hennecke, H. (1991) *Mol. Gen. Genet.* **225,** 38–48.
17. Gilles-Gonzalez, M. A., Gonzalez, G., Perutz, M. F., Kiger, L., Marden, M. & Poyart, C. (1994) *Biochemistry* **33,** 8067–8073.
18. Otwinowski, Z. & Minor, W. (1997) *Methods Enzymol.* **276,** 307–326.
19. Furey, W. & Swaminathan, S. (1997) *Methods Enzymol.* **277,** 590–620.
20. Jones, T. A., Zou, J. Y., Cowan, S. W. & Kjeldgaard, M. (1991) *Acta Crystallogr.* **A47,** 110–119.
21. Brünger, A. T. (1988) *J. Mol. Biol.* **203,** 803–816.
22. Brünger, A. T. (1993) *Acta Crystallogr.* **D49,** 24–26.
23. Laskowski, R. A., MacArthur, M. W., Moss, D. S. & Thornton, J. M. (1993) *J. Appl. Cryst.* **26,** 283–291.
24. McRee, D. E. (1993) *Practical Protein Crystallography* (Academic, San Diego).
25. Kraulis, P. (1991) *J. Appl. Crystallogr.* **24,** 946–950.
26. Merritt, E. & Murphy, M. (1994) *Acta Crystallogr.* **D50,** 869–873.
27. Arents, G. & Love, W. E. (1989) *J. Mol. Biol.* **210,** 149–161.
28. Weichsel, A., Anderson, J. F., Champagne, D. E., Walker, F. A. & Montfort, W. R. (1998) *Nat. Struct. Biol.* **5,** 304–309.
29. Rodgers, K. R., Lukat-Rodgers, G. S. & Barron, J. A. (1996) *Biochemistry* **35,** 9539–9548.
30. Tamura, K., Nakamura, H., Tanaka, Y., Oue, S., Tsukamoto, K., Nomura, M., Tsuchiya, T., Adachi, S., Takahashi, S., Iizuka, T. (1996) *J. Am. Chem. Soc.* **118,** 9434–9435.
31. Winkler, W. C., Gonzalez, G., Wittenberg, J. B., Hille, R., Dakappagari, N., Jacob, A., Gonzalez, L. A. & Gilles-Gonzalez, M. A. (1996) *Chem. Biol.* **3,** 841–850.
32. Mansy, S. S., Olson, J. S., Gonzalez, G. & Gilles-Gonzalez, M. A. (1998) *Biochemistry* **37,** 12452–12457.
33. Bertolucci, C., Ming, L.-J., Gonzalez, G. & Gilles-Gonzalez, M. A. (1996) *Chem. Biol.* **3,** 561–566.
34. Quillin, M. L., Arduini, R. M., Olson, J. S. & Phillips, G. N. (1993) *J. Mol. Biol.* **234,** 140–155.
35. Olson, J. S. & Phillips, G. N. (1997) *J. Biol. Inorg. Chem.* **2,** 544–552.
36. Perutz, M. F. (1970) *Nature (London)* **228,** 726–739.
37. Perutz, M. F. (1989) *Mechanisms of Cooperativity and Allosteric Regulation in Proteins* (Cambridge University Press, Cambridge, U.K.).
38. Blanco, G., Drummond, M., Woodley, P. & Kennedy, C. (1993) *Mol. Microbiol.* **9,** 869–879.
39. Leong, D., Pfeifer, F., Boyer, H. & Betlach, M. (1988) *J. Bacteriol.* **170,** 4903–4909.
40. Kabsch, W. & Sander, C. (1983) *Biopolymers* **22,** 2577–2637.
41. Eich, R. F., Li, T., Lemon, D. D., Doherty, D. H., Curry, S. R., Aitken, J. F., Mathews, A. J., Johnson, K. A., Smith, R. D. & Phillips, G. N. (1996) *Biochemistry* **35,** 6976–6983.